UNIVERSITY OF CALIFORNIA, SAN DIEGO

Anti-tumor effects in head and neck cancer in response to toll-like receptor activation, checkpoint inhibition, and chemotherapy

A Thesis submitted in partial satisfaction of the requirements for the degree
Master of Science

in

Biology

by

Shannon Shueyin Zhang

Committee in charge:

Professor Dennis A. Carson, Chair
Professor Gen-Sheng Feng, Co-Chair
Professor Li-Fan Lu

2016

The Thesis of Shannon Shueyin Zhang is approved, and it is acceptable in quality and form for publication on microfilm and electronically:

_____

_____

Co-Chair

_____

Chair

University of California, San Diego

2016

DEDICATION

This thesis is dedicated to my family who has been my support system through all moments of my life. Thank you for inspiring me to pursue my passions. To my mother, Aijun Zhang, father, Kuan Zhang, and brother, Brandon Zhang: You three mean the world to me.

EPIGRAPH

Live as if you were to die tomorrow. Learn as if you were to live forever.

Mahatma Gandhi

TABLE OF CONTENTS

LIST OF ABBREVIATIONS

Ab	antibody
ANOVA	analysis of variance
APC	antigen presenting cells
CD	cluster of differentiation
CTL	cytotoxic T lymphocytes
CTLA-4	cytotoxic T lymphocyte-associated protein 4
DAMP	damage associated molecular patterns
DCs	dendritic cells
DMEM	Dulbecco's Modified Eagle Medium
DMSO	dimethyl sulfoxide
FACS	fluorescence-activated cell sorting
FBS	fetal bovine serum
FDR	false discovery rate
FITC	fluorescein isothiocyanate
HLA	human leukocyte antigen
HMGB1	high mobility group box 1 protein
HNC	head and neck cancer
HNSCC	head and neck squamous cell carcinoma
HSP	heat shock protein
IFN	interferon
Ig	immunoglobulin
IL	interleukin
i.p.	intraperitoneal
IRAK	interleukin-1 receptor-associated kinase
i.t.	intratumoral
i.v.	intravenous
mAb	monoclonal antibody
MDSC	myeloid-derived suppressor cells
MHC	major histocompatibility complex
MTEC	mouse tonsil epithelial cells
MyD88	myeloid differentiation primary response 88
NFκβ	nuclear factor kappa beta
NK	natural killer
OVA	ovalbumin
PAMP	pathogen-associated molecular patterns
PD-1	programmed death-1
PD-L1	programmed death-ligand 1
PE	phycoerythrin
P/S	penicillin-streptomycin
Rb	retinoblastoma tumor suppressor protein

ROS	reactive oxygen species
s.c.	subcutaneous
SCC-7	squamous cell carcinoma seven
SEM	standard error of mean
STD	sexually transmitted disease
TAM	tumor-associated macrophages
TGF	transforming growth factor
Th	helper T cells
TIL	tumor infiltrating lymphocytes
T_{regs}	regulatory T cells
Veh	vehicle
WT	wild type

LIST OF FIGURES

LIST OF TABLES

ACKNOWLEDGEMENTS

First and foremost, I would like to express my gratitude to Dr. Dennis Carson, my thesis advisor, for welcoming me into his lab when I was a third year undergraduate student at UCSD. I would also like to thank Dr. Gen-Sheng Feng, my co-chair, and Dr. Li-Fan Lu, my third committee member, for aiding me in my graduate endeavors. My experience in the BS/MS program has taught me to become a critical and scientific thinker.

I would also like to give a special thank you to Dr. Tomoko Hayashi, the project scientist, who has guided me throughout the entire writing process and pushed me to become a proactive leader in the lab. Without her guidance and willingness to help with my thesis, I would not be where I am today.

I would like to extend my thanks to all the members in the Carson laboratory whom I thoroughly enjoyed working amongst. Especially Brian Crain, who patiently trained me in many laboratory techniques, Shiyin Yao and Richard Mathewson, who were always willing to teach and advise me, Dr. Fumi Kaneko, Alast Ahmadi, and Melody Sayrany, who assisted me in many experiments, and the chemists Michael Chan and Howard Cottam, who contributed greatly towards this project. Acknowledgements to Moores Cancer Center Cancer Immunotherapy Foundation funding by Ralph and Fernanda Whitworth.

Last but not least, a warm thank you to my family members Aijun Zhang, Kuan Zhang, and Brandon Zhang, as well as my friends, for their moral support throughout my graduate studies.

ABSTRACT OF THE THESIS

Anti-tumor effects in head and neck cancer in response to toll-like receptor activation, checkpoint inhibition, and chemotherapy

by

Shannon Shueyin Zhang

Master of Science in Biology

University of California, San Diego 2016

Professor Dennis A. Carson, Chair
Professor Gen-Sheng Feng, Co-Chair

Head and neck cancer (HNC) affects approximately 600,000 individuals annually and occurs when squamous cells lining the oral cavity, nasal cavity, and throat become cancerous. Certain problems are associated with current therapies. Surgery can lead to a lower quality of life due to functional and cosmetic disturbances while chemotherapy and radiation have high

toxicity levels. In addition, chemotherapy has low response rates and high recurrence rates. Thus, it is necessary to utilize immune-directed therapies to treat patients in a process called cancer immunotherapy.

In this study, the therapeutic efficacy of combination cancer immunotherapy is studied on murine models inoculated with squamous cell carcinoma VII. The hypothesis is that using a combination of immunotherapeutic methods and standard treatment can lead to smaller sizes of local, distant, and subsequent tumors. In this study, the immune system is activated and enhanced through the activation of toll-like receptors (TLRs) and the inhibition of immune checkpoints. Treatment methods including TLR7 activation with a 1V270 ligand, TLR9 activation with a SD-101 ligand, checkpoint inhibition with an anti-PD-1 monoclonal antibody, chemotherapy drug, cisplatin, and combination approaches were tested. When used in conjunction with anti-PD-1 agent, 1V270 and SD-101 both showed a reduction in growth on local, distant, and subsequent tumors. 1V270 with cisplatin showed a reduction in growth on local and subsequent tumors. Upon further investigation of the infiltrating cells in the tumor microenvironment by FACS, the combination therapy of 1V270 with cisplatin or anti-PD-1 agent provided higher anti-tumor M1 macrophage to pro-tumorigenic M2 macrophage ratio.

INTRODUCTION

Head and Neck Cancer

Approximately 1.7 million individuals are diagnosed with cancer annually in the United States[1]. As observed in other types of cancers, genetic and environmental factors are known to induce head and neck cancer (HNC), the 6th most common type of cancer[1]. HNC emerges in areas such as the sinuses, oral cavity, nasal cavity, and throat, where squamous cells located in mucous membranous areas become cancerous[1]. Because HNC is located around the head and neck areas, patients often experience pain, numbness, lumps, and bleeding in the affected areas and can develop difficulty swallowing, speaking, and/or breathing[1]. Risk factors of HNC include genetic factors, habitual alcohol and/or tobacco use, poor oral hygiene, and the infection of human papillomavirus (HPV) strains 16 or 18 upon oral sex transmission[1]. Due to the high prevalence of HPV, now the most common sexually transmitted disease (STD), up to 70% of all oropharyngeal cancers are due to HPV infections[2].

Problems with Current Treatment in Head and Neck Cancer

Because HNC affects multiple organs around the head and neck regions, the tumors evolved are often heterogeneous in nature, leading to difficult diagnosis and treatment procedures[3]. The tumors are harder to diagnose because a small portion of the tumor taken for a biopsy may misrepresent the entire tumor[4]. There is also a high recurrence probability after treatment because the diverse tumor cells may not all respond to treatment as expected[4]. With multiple different risk factors associated with HNC, different patients may also respond differently to treatment methods. Current methods to treat HNC include chemotherapy, surgery, and radiation[1]. Chemotherapy can be used when the cancer cells have metastasized while surgery and radiation are used to treat localized tumors. When patients are treated with surgery in the head and neck regions, functional and cosmetic disturbance are often a result

because many vital organs used daily such as the tongue, nose, and throat can become affected[5]. Treatment with radiation and chemotherapy, on the other hand, are associated with high toxicity levels[6]. Single agent chemotherapy has a fairly low response rate of 15% to 43% in HNC[7]. Furthermore, in previously treated HNC patients, 30%-40% develop locoregional cancer while 20%-30% develop metastatic cancer[7]. Due to the low response rates and moderately high recurrence rates, it is necessary to turn to the body's own immune system in addition to current treatments to fight HNC in a process called cancer immunotherapy.

Immuno-chemotherapy

Immunotherapy and chemotherapy can be used together in a process called immuno-chemotherapy. In this mechanism, chemotherapy kills cancer cells causing them to release tumor-specific antigens that are recognized as non-self by innate immune cells such as dendritic cells (DCs)[8]. Tumor-specific antigens are abnormal molecules that are produced by tumor cells due to a mutation which normal cells do not express[9]. In the case of HPV^+ HNC, oncogenic E6 and E7 viral proteins can be recognized as foreign and targeted[6]. E6 and E7 proteins expressed in HPV inhibit tumor suppressors p53 and Rb, both regulators of the cell cycle, respectively[10]. Simultaneously, the dying cancer cells release danger associated molecules such as heat shock proteins (HSPs) and high mobility group box 1 protein (HMGB1) that activate DCs to increase the uptake of antigen molecules and the antigen cross presentation process[11]. After DCs present antigens to T cells during the priming phase, the activated antigen specific T cells and other activated immune cells attack the tumor cells[12]. Although this process naturally occurs in patients treated with chemotherapy, it is important to elevate the immune system at a higher level and use a lower dose of chemotherapy for immuno-chemotherapy. This is because chemotherapy is a nonspecific treatment that can target and kill immune cells. In addition, tumor cells also exhibit immunosuppressive

strategies. In recent reports, low dose chemotherapy used in combination with certain toll-like receptors (TLRs), TLR7 (Imiquimod) and TLR9, were evident to be effective in clinical trials[13]. Whereas current methods directly target present cancer cells, they do not play a role in preventing recurrent tumors from forming. Activation of the immune system, on the other hand, has the potential to inhibit recurring tumors from forming if an adaptive response is initiated. Cisplatin is one commonly used chemotherapeutic drug that is used in this project[14]. Cisplatin is able to enter the nucleus of cancer cells where its chloride ligands are displaced by water due to the concentration gradient. Nitrogen from the guanine bases in DNA then crosslink to cisplatin as they displace water causing mitosis interference and eventual apoptosis[14].

Immune Status of Tumor Microenvironment of Head and Neck Cancer

It is important to boost the immune system when combatting HNC because tumor cells often exhibit immunosuppressive strategies[15]. Tumor cells can inhibit T cell activation, differentiation, and proliferation by secreting factors such as interleukin 10 (IL-10) and tumor growth factor beta (TGF-β)[15]. Although TGF-β exerts tumor suppressor effects in normal cells, it promotes the progression of cancer in tumor cells[16]. IL-10, on the other hand, is a naturally anti-inflammatory cytokine that can inhibit the activity of T cells, natural killer (NK) cells, and macrophage cells to prevent tissue damage[17]. Tumor cells are also able to cause T cell inactivation and apoptosis through their expression of programmed death-ligand 1 (PD-L1), which is activated when bound to its receptor, programmed death-1 (PD-1), on tumor-specific T cells. Aside from affecting T cells, which are important effector cells that target tumor cells, tumor cells can also invade bone marrow to disrupt immune cell development and down-regulate major histocompatibility class I (MHC I) and human leukocyte antigen (HLA) expression to evade the host immune system[18]. Evidence also suggests that normal cells

localized in the tumor environment in HNC favor tumor growth and promote angiogenesis[18]. Patients with HNC have less lymphocytes and more regulatory T cells (T_{regs}), a subset of T cells that suppress the immune system for regulation purposes, than unaffected individuals[18]. Due to all the negative effects that tumor cells can exhibit on the immune system, it is important to enhance the immune system for an effective immuno-chemotherapy mechanism.

The Tumor Microenvironment

Before discussing specific immunotherapeutic methods in combatting cancer, it is important to understand the tumor microenvironment, or the cellular environment that localizes within the tumor sites. Tumor-associated macrophages (TAM) are macrophages that reside within the proximity of tumors and affect tumor growth[19]. TAM is not a uniform population and consists of distinct functional populations and intermediates[19]. Simply put, two types of macrophages, the classical M1 macrophage and the alternative M2 macrophage, are present[19]. Certain pathogen associated molecular patterns (PAMPs) including TLR ligands and cytokines such as interferon gamma (INFγ) and interleukins (IL) in the environment cause macrophages to polarize into either M1 or M2[19]. Upon IFNγ stimulation, macrophages polarize to M1 macrophages; upon IL-4 stimulation, macrophages polarize to M2 macrophages[20]. TAM are identified by surface markers as $CD45^{+}CD11b^{+}F4/80^{+}$, M1 macrophages are identified by MHC class $II^{high}CD206^{low}$, and M2 macrophages are identified by MHC class $II^{low}CD206^{high}$[21]. M1 macrophages phagocyte tumor cells and produce effector molecules to eliminate tumor cells[22]. They can present tumor antigens to T cells for tumor-specific adaptive immune responses[22]. Functionally, M1 macrophages help with antitumor immunity whereas M2 macrophages promote wound healing and pro-tumorigenic effects by promoting angiogenesis and inhibiting type 1 T helper cell (Th1) responses[19]. Aside from M2 macrophages, myeloid-derived suppressor cells (MDSC) and T_{regs} are regulatory immune cells

that exhibit immunosuppressive strategies to promote tumor growth[23]. Thus, in addition to immune activation strategies, more research should also be directed towards the downregulation of these immunosuppressive immune cells in the tumor microenvironment.

Toll-like Receptors

TLRs are receptors that are located on innate immune cells such as DCs[24]. There are a total of thirteen TLRs that can each recognize different PAMPS or damage associated molecular patterns (DAMPS) which serve as ligands to generate an immune response[25]. TLR activation can lead to the release of pro-inflammatory cytokines that activate tumor infiltrating immune cells. TLR7, unlike TLR2 or TLR4, are expressed only on a limited amount of cells including DCs, plasmacytoid cells, and B cells[26]. Thus, using ligands that target TLR7 will only affect tumor infiltrating immune cells, leading to a less chance of off-target effects. Frenzel and colleagues confirm the importance of TLR7 activation in combatting cancer, specifically, squamous cell carcinoma (SCC)[27]. When dendritic cells, which serve as the first line of defense, were exposed to head and neck squamous cell carcinoma (HNSCC), they expressed more TLR7 in comparison to other TLRs[27]. The success in activating TLR7 in cancer therapy was confirmed by Hayashi and colleagues when synthetic TLR7 ligand agonist, 1V270, was shown to successfully suppress the growth of melanoma tumors[28]. 1V270, which was used in this project, is a synthetic ligand synthesized by UCSD that is composed of the TLR7 ligand conjugated to a phospholipid moiety[29]. 1V270 has many advantages over a TLR7 ligand alone in its utilization including its high immunopotency, ease in synthesizing large amounts, stability for at least six months, resistance to the heat and cold, and local on-site targeting efficiency[29]. In addition to TLR7 activation, TLR9 activation was also studied in this project because previous studies have shown that TLR9 agonists can cause anti-tumor effects through activating and maturating DCs and aiding in the differentiation of B

cells[30]. Thus, a TLR9 ligand agonist, SD-101, created by Dynavax CA, was studied in combination with other methods[31]. Both TLR7 and TLR9 pathways utilize the myeloid differentiation primary response 88 (Myd88) dependent pathway, in which the adaptor protein Myd88 recruits interleukin-1 receptor-associated kinase (IRAK) which eventually leads to the production of IFN-α and the nuclear localization of the transcription factor nuclear factor kappa beta (NF-κβ), leading to the expression of cytokines[32].

Checkpoint Inhibition

Although the immune system is important in maintaining the health of an individual, it can also lead to detrimental symptoms if it is active at too high of a level[33]. Excessive activation of immune cells and/or chemokine release can cause tissue damage, systemic shock, auto-immune diseases, and even lethality[33]. Thus, a negative feedback by checkpoints exists in the immune system and acts as a homeostatic mechanism to prevent an over-activation of the immune system[34]. Blocking these immune negative feedback systems could enhance tumor-specific immunity and sustain effector T cell activation. Two main sources of immune checkpoints have been utilized for the development of cancer immunotherapy agents: the cytotoxic T lymphocyte-associated protein 4 (CTLA-4) system that acts mainly in the priming phase, where antigen presenting cells (APCs) activate effector immune cells, and the programmed death-1 (PD-1) system that acts mainly in the periphery phase, where activated effector immune cells target tumor cells[35]. The CLTA-4 receptor found on T cells can bind to either B7-1 or B7-2 ligands on APCs to inhibit the proliferation and activation of T cells[36]. The PD-1 on T cells can bind to PD-L1 in tumor cells or APCs and this interaction also inhibits the proliferation and activation of T cells[35]. In treating cancer, it is expected that by blocking the immune checkpoints via antibodies, the immune system will be elevated leading to antitumor properties. In this experiment, an anti-PD-1 antibody is used to block anti-PD-1

from binding to its ligand, anti-PD-L1. In some cases, targeting of the PD-1 system is preferred over targeting of the CTLA-4 system because the CTLA-4 receptor acts early in the priming phase and if blocked, can lead to undesired autoimmune problems[37].

Preclinical Models of HNC

There are different types of HNSCC induced tumors that require different treatment approaches. Thus, it is important to study different HNC models such as HPV$^-$ SCC-7 cells, HPV$^-$ MEER cells, and HPV$^+$ MEER cells (Table 1). SCC-7 cells are poorly immunogenic squamous cells derived spontaneously from an abdominal wall tumor of a C3H mouse; they grow very rapidly in C3H mice[38]. MEER cells are modified forms of mouse tonsil epithelial cells (MTEC) derived from wild type C57BL/6 mice[39]. HPV$^-$ MEER cells are derived from H-Ras transduced MTECs and grow at a moderate rate in C57BL/6 mice[39]. The additional Ras expression allows for immortality of the cells as the Ras protein normally functions to promote cell growth, differentiation, and survival. HPV$^+$ MEER cells additionally include the expression of HPV E6/7 antigens from HPV16 which increases immunogenicity[40]. These cells grow slowly and exhibit strong anti-tumor immune responses. In this project, the HPV$^-$ SCC-7 model is studied in C3H mice specifically.

Table 1: Preclinical cell models in head and neck cancer study. The following table shows three different cell models that reflect head and neck cancer derived from the abdominal wall of C3H or the tonsils of C57BL/6 mice. The HPV$^-$ SCC-7 cell model is used in this project.

Model	**SCC-7**	**HPV$^-$ MEER**	**HPV$^+$ MEER**
Background	C3H(H-2K^k,1-A^k)	C57BL/6 (H-2K^b, 1-A^b)	C57BL/6 (H-2K^b, 1-A^b)
Cell type	Abdominal wall squamous cells	Tonsil epithelial cells	Tonsil epithelial cells
HPV status	-	-	+ (E6/7)
Growth in vivo	Fast	Moderate	Slow

Hypothesis and Experimental Approaches

As a part of the cancer immunotherapy approach, systemic TLR treatments have been performed in several clinical trials. However, due to the systemic adverse effects such as cytokine storm, the repeated treatments were not well tolerated[41]. Local intratumoral (i.t.) treatments with TLR ligands have been widely accepted including topical applications with Imiquimod, which showed therapeutic efficacy[13]. We have previously published that i.t. administration of 1V270 reduced B16 melanoma growth and IL-2 treatment additively improved therapeutic effects of 1V270. Therefore, the hypothesis for this study is that i.t. treatment of 1V270 is able to suppress tumor growth of SCC-7 low immunogenic syngeneic cell line. Since the stimulation upregulated PD-L1 expression on APCs, anti-PD-1 agents were combined with i.t. treatment with 1V270 and therapeutic efficacy was monitored. Cisplatin is widely used for low dose immuno-chemotherapy so it was also used in combination with TLR activation to view effects on tumor size. Finally, tumor infiltrating cells were studied by FACS analysis to discover the mechanism of action. I hope to discover an optimal treatment and administration schedule that will provide for a better therapeutic method in treating HNC with an abscopal effect in a clinical setting.

MATERIALS AND METHODS

Animals

Wild type female C3H/HeOuJ mice were obtained from the Jackson Laboratory (Bar harbor, MA). The UCSD Institutional Animal Care and Use Committee approved all procedures carried out in this study (Protocol numbers S00028 and S05016).

Cell Lines and Reagents

TLR7 ligand phospholipid conjugate, 1V270, was synthesized in our laboratory[42]. TLR9 ligand, SD-101, was provided by Dynavax Technologies Berkeley, CA[43]. RPMI 1640 medium (Invitrogen, Carlsbad, CA) was supplemented with 10% fetal bovine serum (FBS) (Omega Scientific, Inc. Tarzana, CA) and penicillin-streptomycin (P/S) (Life Technologies, Grand Island, NY) (complete RPMI). HPV^- SCC-7 cells were kindly gifted by Dr. John Lee (Sanford Research, SD). SCC-7 cells were cultured in RP10 medium. Endotoxin levels of these drugs were determined by Endosafe® (Charles River Laboratories, Wilmington, MA) and were less than 10 EU/μmol.

Preclinical Models Using SCC-7 Treatment

For the HPV^- HNSCC model, $1X10^5$ SCC-7 tumor cells were subcutaneously (s.c) inoculated in C3H/HeOuJ mice. Intratumoral (i.t.) treatment with 1V270 was initiated on day 8 post inoculation when the diameter of the tumors reached 2-5 mm. Treatment with 1V270 [100 μg (93 nmol/injection)] was administered daily for five consequent days unless otherwise noted. SD-101 (50 μg/injection) was administered on days 7, 11, 14, and 18 post inoculation. The monoclonal antibody (mAb) against murine PD-1 (RMP1-14 clone, BioXcell) (250 μg/injection) was given through intraperitoneal (i.p.) routes. Cisplatin (5 mg/kg) was i.p. administered on days 8 and 12. Tumor lengths and widths were recorded over days post

inoculation and tumor volumes were calculated using the formula $\frac{width\ x\ width\ x\ length}{2}$. Details of treatment schedules are stated in the figure legends.

RNA Isolation and Nanostring Assay

To study upregulated genes in the tumor microenvironment, tumor tissues were harvested and RNA was isolated using the RNA Isolation Kit: RNeasy Mini Kit per the Qiagen® protocol. RNA samples were stored in -80°C and sent to Nanostring Technologies® to probe for RNA present in tumor cells following the nCounter® Gene Expression Assay protocol.

Analysis of Tumor Infiltrating Lymphocytes

Tumors were cut into small pieces and single cell suspensions were prepared according to the mouse Tumor Dissociation Kit (Miltenyi Biotec SD) using gentleMACS™ Octo Dissociator with Heaters according to the manufacture's protocol (Miltenyi Biotec). Single cell suspensions of tumor cells were stained for 20 min at 4 °C with the following monoclonal antibodies (mAbs) (Table 2).

Table 2: Antibodies chart for FACS staining to detect M1 macrophages, M2 macrophages, and $CD8^+$ T cells in the tumor microenvironment.

Antibody	**Cells**	**Clone**	**Color**	**Company**
CD3ε	T cell	145-2c11	APC	eBioscience
CD8α	T cell	53-6.7	FITC	BD Biosciences
CD11b	Macrophage	M1/70	eFluor 450	eBioscience
CD45	Hematopoietic cells	30-F11	PE/Cy7	BioLegend
F4/80	Macrophage	BM8	APC	eBioscience
Class II (I-Ek)	M1 Macrophage	14-4-4S	FITC	eBioscience
CD206	M2 Macrophage	C068C2	PE	BioLegend
IFNγ	T cell	XMG1.2	APC	eBioscience

After staining, cells were fixed in BD Cytofix/Cytoperm. Data were acquired on FACS

CantoII (Becton Dickinson) and analyzed using FlowJo 10 software (TreeStar Software, Ashland, Oregon).

Graphing of Data and Statistical Significance Analysis

Data were plotted on graphs using Prism software (version 6.0, GraphPad Software, Inc., San Diego, CA) and fitted by nonlinear regression. Analysis of variance (ANOVA) was used to test for the variance among data points. A two tailed student t test or one-way ANOVA with Bonferroni's post hoc or Dunnett's post hoc test was utilized. Survival curves of the mice followed the Kaplan-Meier model and were assessed by log rank tests for statistical significance. P values lower than 0.05 were considered statistically significant.

RESULTS

Optimal dose of intratumoral 1V270 administration is 100μg per inoculated site

Before different combination therapy methods were assessed, a preliminary study was conducted to test for a dose of 1V270 injection that can induce the suppression of SCC-7 tumor growth. Groups of eight wild type (WT) female C3H/HeOuJ mice were s.c. inoculated with $1x10^5$ SCC-7 on their right flanks on day 0 and treated with different doses of 1V270 daily from days eight through twelve to determine the optimal dose (Figure 1a). In a previous study, it was discovered that 3μg of 1V270 was enough to inhibit tumor growth in a B16 melanoma model[28]. Thus, low doses (8μg or 16μg) of 1V270 were first injected into mice models and tumor sizes were measured. A vehicle group of mice was treated with 9% DMSO in sterile saline i.t. The results show that the three groups of mice did not show a significant difference in tumor growth, indicating that a higher dosage of 1V270 was required to produce an anti-tumor effect (Figure 1b left panel). In a subsequent study, 35μg and 100μg of 1V270 were tested against a vehicle group. Mice treated with 100μg of 1V270 i.t. after SCC-7 inoculation exhibited significantly reduced tumor sizes when compared to the vehicle group ($p<0.05$) while mice treated with 35μg of 1V270 did not (Figure 1b right panel). Thus, 100μg of 1V270 dosage was used in all subsequent experiments.

Optimal frequency of intratumoral 1V270 administration is daily

After determining that the optimal dosage of 1V270 is 100μg per inoculation site, the next preliminary experiment was performed to determine the optimal schedule of 1V270 administration. In a concept called TLR tolerance, cells may become unresponsive with repeated exposure to TLR activation due to physiological regulation purposes[44]. Thus, daily administration of 1V270 was tested against two injections per week to determine which

schedule produced a more anti-tumor effect. Two groups of mice were inoculated with $1x10^5$ SCC-7 s.c. on their right flanks on day 0: one group of fifteen mice was treated with 100μg 1V270 i.t. on days 8, 9, 10, 11, and 12 while another group or fourteen mice was treated with 100μg 1V270 i.t. on days 8, 11, 14, 17, and 20 (Figure 2a). Tumor sizes were assessed and it was seen that as expected, the vehicle group exhibited the largest tumor sizes (Figure 2b). Although mice injected twice a week showed significantly lower tumor sizes when compared to the vehicle group ($p<0.05$), mice injected daily showed an even more significant decrease in tumor sizes when compared to the vehicle group ($p<0.0001$) (Figure 2b). Mice treated with 1V270 daily also exhibited significantly higher survival rates than the vehicle group while mice treated twice a week did not ($p<0.05$) (Figure 2c). Thus 1V270 was injected daily on days 8 through 12 in all subsequent experiments.

Genes related to antigen presentation, PD-L1 and granzyme B are upregulated by 1V270

To elucidate the molecular effects of 1V270 in the tumor cells and the microenvironment, the expression levels of inflammatory and cancer-related genes in the tumor tissue were determined using nCounter® PanCancer Immune Profiling Panel from the NanoString Technologies. Mice were s.c. inoculated with $1x10^5$ SCC-7 on their right flanks on day 0 and treated with 100μg 1V270 i.t. on days 8, 9, 10, 11, and 12. On day 13, tumors were harvested and RNA was extracted using Qiagen Miniprep Kits per protocol (Qiagen). RNA samples were sent to NanoString Technologies and genes were hybridized to analyze gene expression. Many genes from various immune pathways were shown to be upregulated in response to 1V270 (Table 3). Because TLR7 activators are strong type 1 IFN inducers, IFN related genes were upregulated as expected. Genes related to the antigen presenting function, including CD86, and related to MHC and antigen presentation were also upregulated. It should be noted that granzyme B and CD274 (PD-L1) were significantly upregulated. The granzyme

B gene expresses a protease that is released by cytotoxic T lymphocytes (CTL) and NK cells to induce apoptosis in target cells[45]. This suggests that CTL and/or NK cells are activated upon 1V270 treatment[46]. Increased expression of PD-L1, expressed on macrophages, DCs, as well as tumor cells, is known to inhibit T cell activation and to induce apoptosis of effector T cells after ligation with PD-1 on T cells[35]. This finding served as the foundation for the hypothesis that blockage of PD-1 and PD-L1 ligation can produce anti-tumor effects. Therefore, the addition of anti-PD-1 mAb to block the PD-1/PD-L1 interaction was evaluated.

Treatment of 1V270 with anti-PD-1 reduces local and distant tumor sizes

After the preliminary experiments of single dose 1V270 therapy, 1V270 was tested in combination with anti-PD-1 mAb. Four groups of ten mice were inoculated with $1x10^5$ SCC-7 s.c. on their right flanks: one group of mice was treated with 100μg 1V270 i.t. on days 8, 9, 10, 11, and 12, a second group was treated with anti-PD-1 mAb i.p. on days 6, 10, 14, and 18, a third group was treated with a combination of both, and a fourth vehicle group was treated with sterile saline i.t. on days 8, 9, 10, 11, and 12 and rat IgG2a i.p., the isotype for anti-PD-1, on days 6, 10, 14, and 18 (Figure 3a). Tumor sizes were recorded and tumor volumes were calculated and graphed. Figure 3b shows that the combination approach showed a significant reduction in tumor sizes when compared to the vehicle group ($p<0.05$) while 1V270 treated mice did not show significantly reduced tumor sizes when compared to the vehicle mice (Figure 3b). All treatment groups had significantly higher survival rates than the vehicle group (Figure 3c). The survival curve indicated that the combination approach led to about 40% of surviving mice on day 35 while for the other groups, almost all mice were deceased by day 35 (Figure 3c) indicating that the combination approach is preferred over 1V270 alone or anti-PD-1 antibody alone. To evaluate the abscopal effects on distant site tumors, the same protocol was adopted in a second study except both left and right flanks were inoculated with

SCC-7 and only the right tumors were treated with 1V270 (Figure 3a). Single agent treatment of 1V270 and anti-PD-1 agent showed modest reduction of tumor growth (Figure 3d) in the injected site. The combination therapy significantly improved the therapeutic effects compared to the single agent therapy ($p<0.05$) (Figure 3d). On the uninjected site, 1V270 showed almost no effect while tumor growth was significantly suppressed when combined with the anti-PD-1 agent compared to the vehicle group ($p<0.001$) (Figure 3e).

Treatment of SD-101 with anti-PD-1 reduces local and distant tumor sizes

TLR7 and TLR9 are located on intracellular endosomal compartments in immune cells and recognize nucleic acids, signaling exclusively via the MyD88 dependent pathway[47]. TLR7 and TLR9 ligands induce similar cytokine profiles. However, notable differences are observed between the activation of TLR7 and TLR9 in the downstream signaling[48]. Therefore, we studied whether TLR9 activation by SD-101 would exhibit similar effects in the reduction of tumor sizes in comparison to TLR7 activation. Four groups of eight mice were inoculated with $1x10^5$ SCC-7 s.c. on their right and left flanks: one group of mice was i.t. treated with 50μg SD-101 on days 7, 11, 14, 18, and 20, a second group was treated with 250μg anti-PD-1 mAb i.p. on days 4, 6, 11, 14, and 18, a third group was treated with both, and a fourth vehicle group was treated with saline i.t. and rat IgG2a i.p. (Figure 4a). SD-101 was administered on only the right tumors. In the right tumors, the single agent treatment with SD-101 as well as the combination treatment of SD-101 and anti-PD-1 agent showed a significant reduction in tumor sizes than the vehicle group ($p<0.05$) (Figure 4c). In the left untreated tumors, there were significantly smaller tumors only with the combination approach when compared to the vehicle group ($p<0.0001$) but not in the single agent treatment with SD-101 or anti-PD-1 agent (Figure 4c). Upon statistical analysis, all three treated groups of mice had significantly higher survival rates than the vehicle group (Figure 4d). However, mice treated with the combination

approach had the highest survival rate with 20% remaining alive by day 40 while mice in all other groups were deceased by day 30 (Figure 4d).

Treatment of anti-PD-1 with1V270 or SD-101 reduces subsequent tumor sizes

A challenge experiment was then conducted to evaluate if the combination therapy of anti-PD-1 agent with 1V270 or SD-101 can induce an adaptive immune response to lower the tumor sizes of a subsequently administered tumor. Two groups of fifteen mice was inoculated with $1x10^5$ SCC-7 s.c. on their right flanks and treated with 100μg 1V270 i.t. on days 8, 9, 10, 11, and 12 and anti-PD-1 mAb i.p. on days 6, 10, 14, and 18 or 50μg SD-101 on days 7, 11, 14, 18, and anti-PD-1 mAb i.p. on days 4, 6, 11, 14, and 18 (Figure 5a). An age-matched group of naïve mice was used for a positive control to visualize the normal growth pattern of tumors without pre-exposure to SCC-7 or treatment (Figure 5a). All three groups were challenged with $1x10^5$ SCC-7 s.c. on their left flanks. Tumor sizes were recorded and tumor volumes were calculated and graphed. Mice that were previously exposed to SCC-7 cells and 1V270 or SD-101 and anti-PD-1 treatment grew significantly smaller tumors than the naïve mice ($p<0.05$) (Figure 5b). This data indicates that tumor bearing mice treated with the combination therapy developed a tumor-specific adaptive immune response.

1V270, anti-PD-1, and a combination increase M1/M2 macrophage ratio in the tumor microenvironment and $CD8^+$ T cell population in the spleen

TLR stimulation promotes rapid macrophage maturation of monocytes[49]. Anti-PD-1 agent is hypothesized to increase the M1 polarization of macrophages induced by TLR ligand[56]. To test how 1V270 and anti-PD-1 alter the macrophage phenotypes in the tumor microenvironment, tumor samples were harvested on day 21 to assess tumor infiltrating macrophages by FACS after following protocol in figure 3a with sample sizes of four. In the

macrophage population, M1 macrophages are MHC class $II^{high}CD206^{low}$ and M2 macrophages are MHC class II^{low} $CD206^{high}$[21]. Macrophages were identified as $CD45^{+}CD11b^{+}F4/80^{+}$ gated population. It appeared that treatment with the anti-PD-1 agent causes an increase in the M1 macrophage population in the tumor infiltrating macrophage population (39.7%) when compared to the effects by 1V270 (29.4%) and even more so when compared to the effects in the vehicle group (14.3%) (Figure 6a). The population of M1 macrophage out of total macrophages in the tumor microenvironment was similar between anti-PD-1 alone treatment and the combination treatment of 1V270 and anti-PD-1 (38.3%) (Figure 6a). The M2 macrophage population in the tumor infiltrating macrophage population decreases from the vehicle group (45%) to 1V270 treated group (19.1%) to the anti-PD-1 treated group (12.1%) (Figure 6a). The M2 population in the tumor microenvironment was similar between anti-PD-1 and combination group (10.5%) (Figure 6a). Gene expression analysis by Nanostring Assay indicated that 1V270 treatment increases the gene expression related to the antigen presenting function of the tumor and the tumor microenvironment. We therefore hypothesized that anti-PD-1 treatment with 1V270 could increase activated antigen specific $CD8^{+}$ T cell population in the tumor microenvironment. Activated $CD8^{+}$ T cells were identified by intracellular expression of IFNg by FACS. $CD8^{+}$ T cells in the tumor infiltrating lymphocyte (TIL) significantly increased by treatment with anti-PD-1 agent in the untreated tumor, and modestly increased by the combination therapy in both side tumors (Figure 6b). $CD4^{+}$ T cell population was significantly increased by the combination therapy in treated and untreated tumors (Figure 6c). Significantly higher activated $CD8^{+}$ T cell population was observed in the spleen from mice treated with the combination therapy (Figure 6d). These data suggests that the combination therapy increases systemic activation of $CD8^{+}$ T cell responses.

Treatment of 1V270 with cisplatin reduces local tumor sizes

With the success of TLR activation and checkpoint inhibition used in combination with each other, the next step was to determine the effects of TLR activation and a standard treatment method, chemotherapy. Four groups of seven mice were inoculated with $1x10^5$ SCC-7 s.c. on their right flanks: one group of mice was treated with 100μg of 1V270 i.t. on days 8, 9, 10, 11, and 12, a second group of mice was treated with the 5mg/kg of cisplatin i.p. on days 8 and 12, a third group of mice was treated with both, and a fourth group of vehicle treated mice received DMSO i.t. and sterile saline i.p. (Figure 7a). All three treatments showed significantly reduced tumor sizes compared to vehicle tumors ($p<0.05$) while the combination approach showed the smallest tumor size (Figure 7b). Survival rates were highest for the combination approach as 40% of mice survived on day 35 while mice from the other groups were deceased by day 35 (Figure 7c). Mice treated with 1V270 alone had significantly higher survival rates than vehicle group ($p<0.05$) while mice treated with 1V270 and cisplatin had even significantly higher survival rates than vehicle group ($p<0.001$).

Treatment of 1V270 with cisplatin reduces subsequent tumor sizes

To evaluate whether the TLR activation and chemotherapy induces a tumor-specific adaptive immune responses, a new group of mice treated with 1V270 and cisplatin were challenged with freshly prepared SCC-7 cells. Mice were inoculated with $1x10^5$ SCC-7 s.c. on their right flanks and then treated with 100μg of 1V270 i.t. on days 8, 9, 10, 11, and 12 and 5mg/kg of cisplatin i.p on days 8 and 12. (Figure 8a). Age-matched naïve mice that were not pre-exposed to SCC-7 and treatment were used for a positive control to visualize the normal growth pattern of tumors. On day 28, both groups of mice were inoculated with $1x10^5$ SCC-7 s.c. on their left flanks (Figure 8a). Tumor size analysis showed that mice previously inoculated with SCC-7 and treated showed significantly reduced subsequent tumor growth compared to the naïve mice ($p<0.05$) (Figure 8b).

1V270, cisplatin, and a combination increase M1/M2 macrophage ratio and $CD8^+$ T cell population in the tumor microenvironment

To evaluate the mechanism of action by which 1V270 and cisplatin reduces tumor growth, the impact of 1V270 and/or cisplatin treatment in the TIL was studied by FACS. Tumor samples were harvested for a FACS plot of tumor infiltrating immune cells. Macrophages were identified as $CD45^+CD11b^+F4/80^+$ gated population[21]. In the macrophage population, M1 macrophages are MHC class $II^{high}CD206^{low}$ and M2 macrophages are identified as MHC class II^{low} $CD206^{high}$[21]. It appeared that in the vehicle treated group, there was a prevalence of 88.8% M2 macrophages and only 0.44% M1 macrophages (Figure 9a). In the cisplatin treated group, there was an increase to 4.65% M1 macrophage and a decrease to 47.4% M2 macrophages. In the 1V270 treated group, the same trend is seen with 3.19% M1 macrophages and 58.2% M2 macrophages. With the combined 1V270 and cisplatin treatment, an additive effect is seen with 7.81% M1 macrophages and 21.8% M2 macrophages (Figure 9a). However, when analyzing for significance, the M1 cell population in the tumor infiltrating macrophage population was not significantly different amongst the treatment groups (Figure 9b). The M2 cell population was significantly lower in the combination treatment group tumor microenvironment when compared to the vehicle group ($p<0.05$) (Figure 9c). Finally, the frequency of $CD8^+$ T cells was analyzed in the tumor microenvironment and it was seen that mice treated with the combination of 1V270 and cisplatin showed significantly enhanced $CD8^+$ T cell frequency ($p<0.05$) while 1V270 alone showed a slight but not significant increase in the $CD8^+$ T cell frequency (Figure 9d). Cisplatin alone did not affect $CD8^+$ T cell frequency.

DISCUSSION

In the preliminary experiments, it was shown that daily i.t. injections of 1V270 improved the outcome of tumor suppression when compared to 1V270 injections twice a week. Daily administration of TLR ligand is known to induce refractoriness against subsequent TLR challenges in TLR tolerance[44]. The reason why we did not see this could be the fact that the injections were local. Thus, new immune cells were being recruited to the tumor microenvironment and stimulated instead of the same immune cells being stimulated repeatedly.

From the results, it seems that as a single agent therapy, SD-101 is able to produce a stronger anti-tumor effect than 1V270 alone in a local tumor. This may be due to the fact that although TLR7 and TLR9 are located in the same region in the cell and produce similar cytokines, the downstream mechanisms between the two are different[48]. Puig and colleagues showed that while TLR7 agonists produce a more rapid and temporary induction of IFN transcripts, TLR9 agonists produce a more sustained and longer induction of IFN transcripts, which may be the reason why TLR9 activation is more effective as cytokine production lasts longer[48].

The combination therapies with TLR ligands, both TLR7 and TLR9, and the checkpoint inhibitor showed significantly reduced tumor growth in untreated sites, indicating that this combination therapy was able to establish a tumor-specific adaptive immune response that had abscopal effects. This finding was further supported by the inhibition of tumor growth of the mice that were previously treated with the combination therapy with 1V270 or SD-101 plus anti-PD-1 agents (Figure 5b). This trend was also seen in the challenge experiment using 1V270 and cisplatin (Figure 8b). In HNC patients, although the incidences of distant metastases are relatively small compared to other malignancies, the distant metastases impair

the survival of patients[50]. This induction of a tumor-specific adaptive immune response provides the potential to further improve patient prognosis by preventing metastasis and recurrence.

Tumor infiltrating macrophages exhibit high plasticity and are divided into a simplified M1-type and M2-type phenotype adapted from Th1 and Th2 paradigms[51]. M1-type macrophages are considered as anti-tumor macrophages and secrete factors inhibiting tumor growth, such as high levels of proinflammatory cytokines (TNF-α, IL-1, IL-6, and IL-12) and increased levels of superoxide anions, oxygen radicals, and nitrogen radicals[52]. Furthermore, M1 macrophages can express high levels of MHC class I and II antigens and secrete complement factors that facilitate complement-mediated phagocytosis[53]. Conversely, M2 macrophages mainly participate in parasite clearance, tissue remodeling, immune modulation, and tumor progression[54]. It was expected that i.t. administration of 1V270 promotes M1 polarization because the activation of TLR signaling pathway is well known to promote monocyte differentiation into the M1 phenotype[55]. Systemic administration with a sub-therapeutic dose of cisplatin (5 mg/kg) may cause tumor cell death in which the DAMPs released could initiate an innate immune activation that potentiates M1 polarization. Previous data suggests that anti-PD-1 therapy is also a main driver that increases M1/M2 ratio. Chen and colleagues found that a deficiency of PD-1/PD-L1 ligation resulted in M1 polarization rather than M2 polarization of macrophages[56]. On the bases of this information, it was believed that the combination therapy with 1V270 and anti-PD-1 agent or 1V270 and cisplatin would further increase the M1 population in the tumor microenvironment. However, the FACS data indicated similar M1 populations in the tumor microenvironment of mice treated with anti-PD-1 therapy alone and 1V270 with anti-PD-1 agent (Figure 6a). The M1 population in the tumor microenvironment of mice treated with 1V270, cisplatin, or both were also not significantly different (Figure 9b). The lack of the difference in the TIL by different treatments

might be due to the timing of the sample collection. In fact, the activated $CD8^+$ T cells were significantly increased in the combination therapy (Figures 6d, 9d). Furthermore, tumor bearing mice treated with combination therapy were refractory to the subsequent SCC-7 challenge (Figures 5b, 8b), strongly suggesting that the combination therapy provided tumor-specific immune protection.

To our best knowledge, there is no report showing that anti-PD-1 agent promotes M1 macrophage polarization. Our data shows that systemic anti-PD-1 agent increased M1/M2 ratio in macrophage population when compared to the vehicle group (Figure 6a). Furthermore, anti-PD-1 treatment primarily increased $CD8^+$ T cell population (Figure 6b). One possible explanation for why anti-PD-1 agent increased M1-type macrophage population may be that activated tumor-specific $CD8^+$ T cells can promote M1 polarization by IFNγ release[57]. The MDSC population was not studied in my project. Because this cell type was presented as a significant negative contribution towards the activation of tumor-specific T cells, contribution of the checkpoint inhibitors TLR ligands or cytotoxic treatment should be studied further.

In the tumor challenge study in this project, naïve age-matched non-tumor bearing mice were used as a positive control. The adaptive immune responses are widely accepted as important players to prevent metastasis or recurrence of solid tumors[58]. The cell types that activate innate lymphoid cells, such as NK cells, have been implicated as contributors to the promotion, maintenance, or elimination of tumors[59]. Currently, an experiment is conducted to include a group of mice without bearing tumors that are treated with 1V270 and anti-PD-1 agents to see if the treatments alone can reduce the growth of a subsequently introduced tumor.

Figure 10 exhibits the current working hypothesis of the mechanism of action by which the combination therapy effectively induces a tumor-specific adaptive immune response. Our data suggests that anti-PD-1 agent works on both the activation of innate immune cells and T cells whereas TLR ligands and cisplatin contribute mainly to innate immune cells. With these effects, the next steps would be to determine the details of the mechanism of action by which $CD8^+$ T cells are studied because these effector cells are previously found to be in high numbers in patients who survive cancer treatment[60]. Similar to the other cancer immune therapy, it is highly possible that the tumor-specific adaptive immune responses are mediated by cytotoxic T cells. Currently, the depletion of $CD8^+$ T cells is tested to see the effects of these immune cells in relation to resistance to subsequent tumor challenge.

In summary, the study revealed that 1) daily intratumoral treatment with 100μg 1V270 significantly suppressed tumor growth of the HPV^- HNC model, 2) combination therapy with the checkpoint inhibitor anti-PD-1 agent additively reduced tumor growth on both treated and untreated tumors, 3) combination therapy with 1V270 and anti-PD-1 agent increased M1-type macrophages and reduced M2-type macrophages, and 4) the challenged tumor growth was slowed in mice treated with the combination therapy. The combination therapy with the ligands for TLR7 or TLR9 with checkpoint inhibitor or chemotherapy will be a promising therapeutic approach to prevent recurrent and distant metastasis in HNC.

FIGURES

A

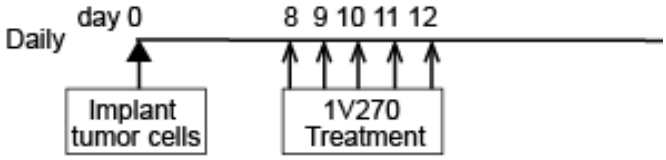

B

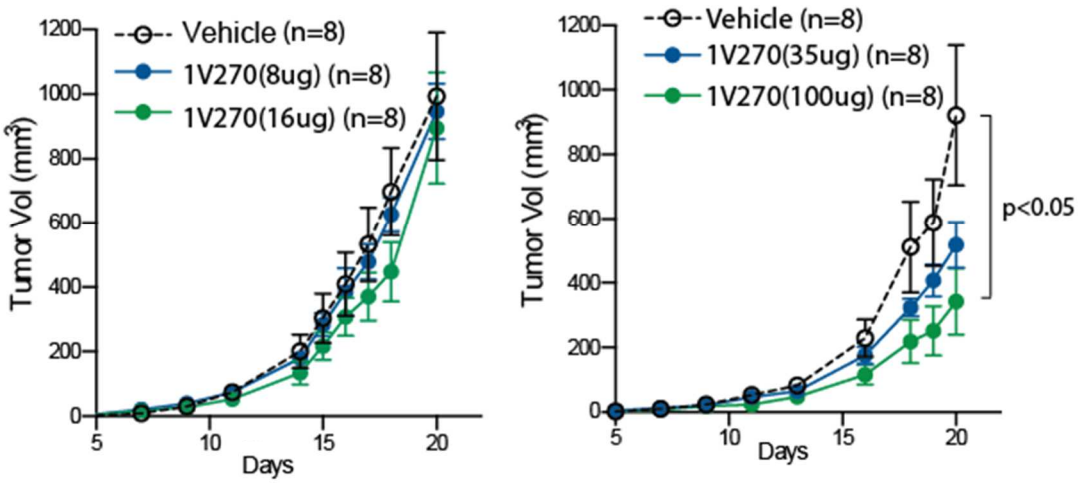

Figure 1: Optimal dose of intratumoral 1V270 administration is 100ug per inoculated site. (A) Treatment protocol. Wild type female C3H/HeOuJ mice (n=8) were inoculated with $1x10^5$ SCC-7 s.c. on right flanks on day 0. 1V270 (8ug or 16ug (left panel), or 35ug or 100ug (right panel)) was administered on days 8, 9, 10, 11, and 12. (B) Tumor lengths and widths were recorded over days post inoculation and tumor volumes were calculated using the formula $\frac{width\ x\ width\ x\ length}{2}$ and graphed using Prism software (version 6.0, GraphPad Software, Inc., San Diego, CA) and fitted by nonlinear regression. p value was calculated using a one-way Anova. p value < 0.05 was considered statistically significant.

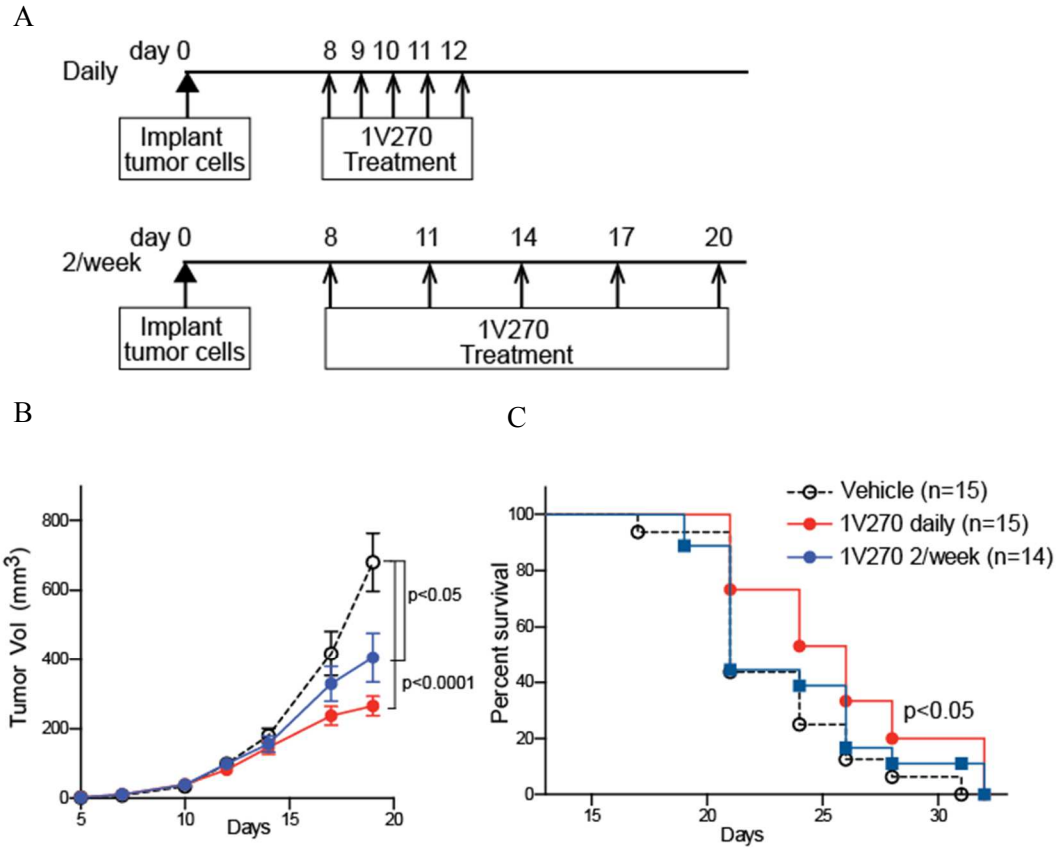

Figure 2: Optimal frequency of intratumoral 1V270 administration is daily. (A) Treatment protocol. Wild type female C3H/HeOuJ mice were inoculated with $1x10^5$ SCC-7 s.c. on right flanks on day 0. 1V270 (100ug) was administered i.t. on days 8, 9, 10, 11, and 12 (n=15) or days 8, 11, 14, 17, and 20 (n=14) to test for optimal administration schedule. A vehicle group was injected with sterile saline i.t. on days 8, 9, 10, 11, and 12 (n=15). (B) Tumor lengths and widths were recorded over days post inoculation and tumor volumes were calculated using the formula $\frac{width\ x\ width\ x\ length}{2}$ and graphed using Prism software (version 6.0, GraphPad Software, Inc., San Diego, CA) and fitted by nonlinear regression. p value was calculated using one-way Anova. (C) Survival curve was graphed using Kaplan-Meier model. p value was calculated using log rank test. p value < 0.05 was considered statistically significant.

Table 3: Genes related to antigen presentation, PD-L1, and granzyme B are upregulated by 1V270. Wild type female C3H/HeOuJ mice were inoculated with $1x10^5$ SCC-7 s.c. on right flanks on day 0. 1V270 (100ug) was administered i.t. on days 8, 9, 10, 11, and 12 or sterline saline was administered i.t. as vehicle. Tumors were collected on day 13 and RNA was extracted and sent to NanoString Technologies for analysis. NanoString data showing key upregulated genes in indicated immune pathways upon 1V270 treatment. p values and adjusted FDR q-values are shown. The p values and FDR q-values were obtained from GSEA software analysis.

Pathway (total # genes)	# significantly upregulated genes[1)]	Nominal p-value[2)]	FDR q-value[3)]	Key upregulated genes in pathway
MHC (29)	19	0.012	0.06	H2-M3, H2-Ob, H2-K1, Ciita
Antigen processing (30)	18	0.078	0.24	Tap1/2, Psmb8, Psmb9, Cd1d2,
IFN (38)	20	0.06	0.19	Ifna1, Irf7, Irgm2, Ifitm1, Ifi35,Ifi44
T cell functions (183)	103	0.008	0.16	Cd3e, Gzmb, CD274, Cd40lg, CCL3
B cell functions (81)	48	0.007	0.2	CD86, CD69, CD19, Ctla4,Ptprc,Syk
[1)] Number of significantly upregulated genes. [2)] Nominal p-value for gene set. [3)] FDR q value for pathway				

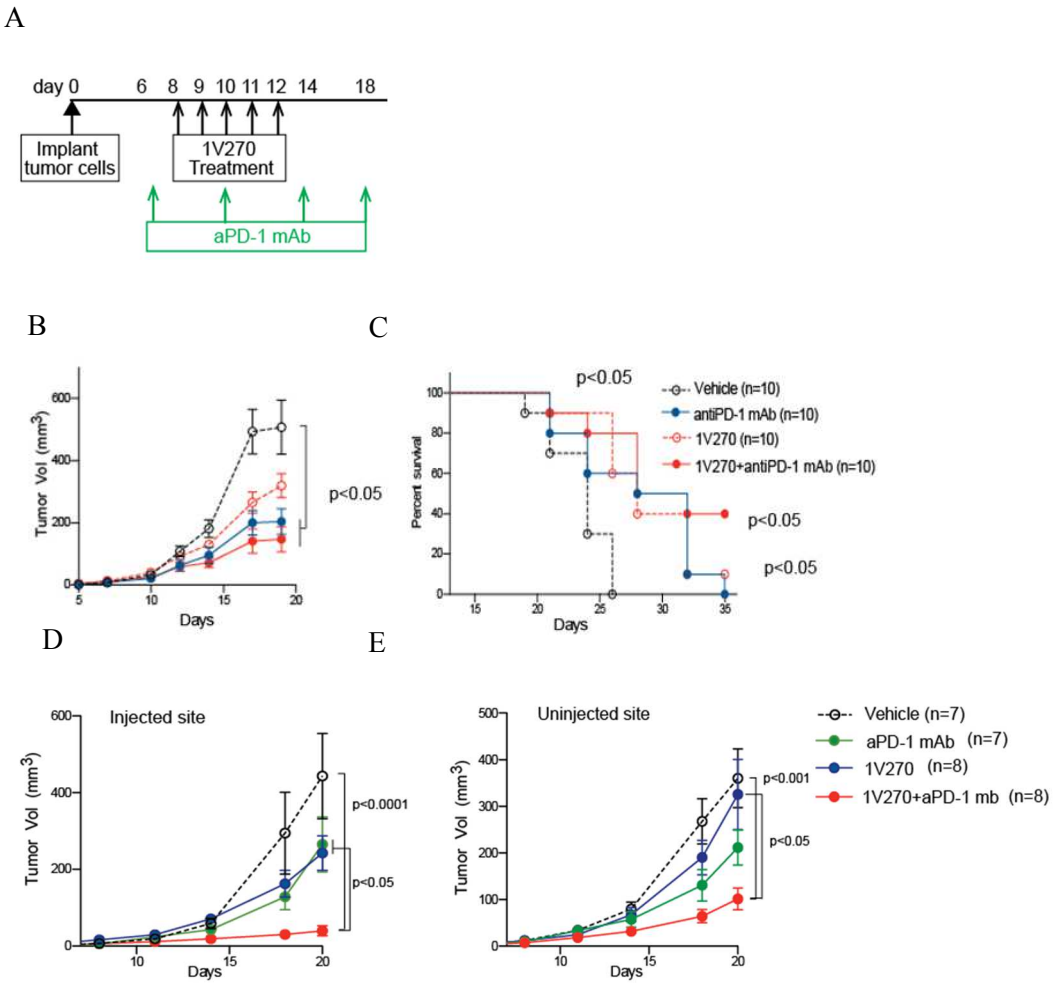

Figure 3: Treatment of 1V270 with anti-PD-1 reduces local and distant tumor sizes**.** (A) Treatment protocol. Wild type female C3H/HeOuJ mice were inoculated with $1x10^5$ SCC-7 s.c. on right flanks on day 0. 1V270 (100ug) was administered i.t. on days 8, 9, 10, 11, and 12 and anti-PD-1 antibody (250ug) was administered i.p. on days 6, 10, 14, and 18. (B) Tumor lengths and widths were recorded over days post inoculation and tumor volumes were calculated using the formula $\frac{width\ x\ width\ x\ length}{2}$ and graphed using Prism software (version 6.0, GraphPad Software, Inc., San Diego, CA) and fitted by nonlinear regression. p value was calculated using one-way Anova. (C) Survival curve was graphed using Kaplan-Meier model. p value was calculated using log rank test. (D) Treated right tumor volumes recorded over days post inoculation of a second group of mice treated as in figure 4a but with SCC-7 inoculation on both flanks. (E) Untreated left tumor volumes recorded over days post inoculation. p value < 0.05 was considered statistically significant.

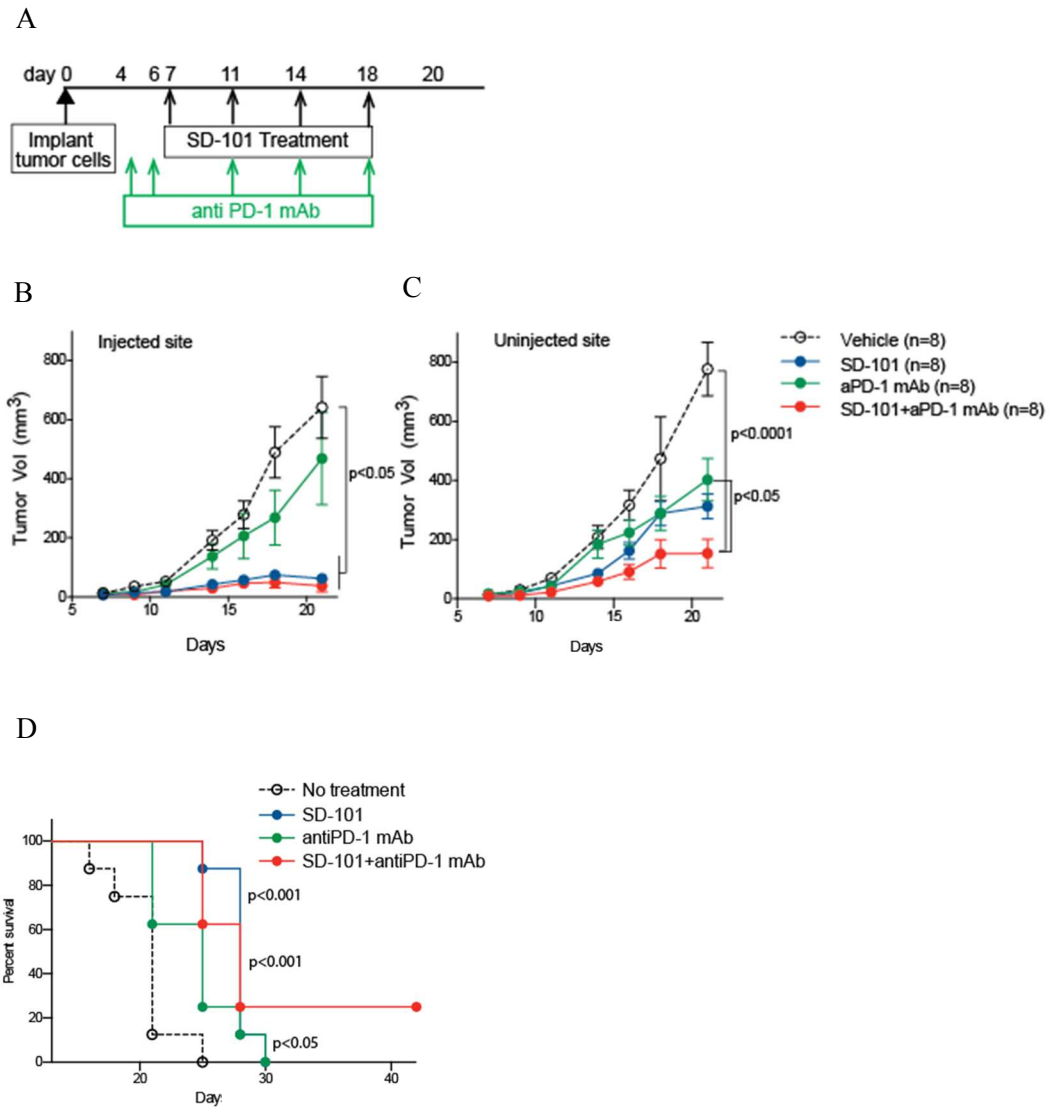

Figure 4: Treatment of SD-101 with anti-PD-1 reduces local and distant tumor sizes. (A) Treatment protocol. Wild type female C3H/HeOuJ mice were inoculated with $1x10^5$ SCC-7 s.c. on their right flanks on day 0. SD-101 (50ug) was administered i.t. on days 7, 11, 14, and 18 and anti-PD-1 antibody (250ug) was administered i.p. on days 4, 6, 11, 14, and 18. (B) Right treated tumor lengths and widths were recorded over days post inoculation and tumor volumes were calculated using the formula $\frac{width\ x\ width\ x\ length}{2}$ and graphed using Prism software (version 6.0, GraphPad Software, Inc., San Diego, CA) and fitted by nonlinear regression. p value was calculated using one-way Anova. (C) Left untreated tumor volumes were calculated using the same formula. (D) Survival curve was graphed using Kaplan-Meier model. p value was calculated using log rank test. p value < 0.05 was considered statistically significant.

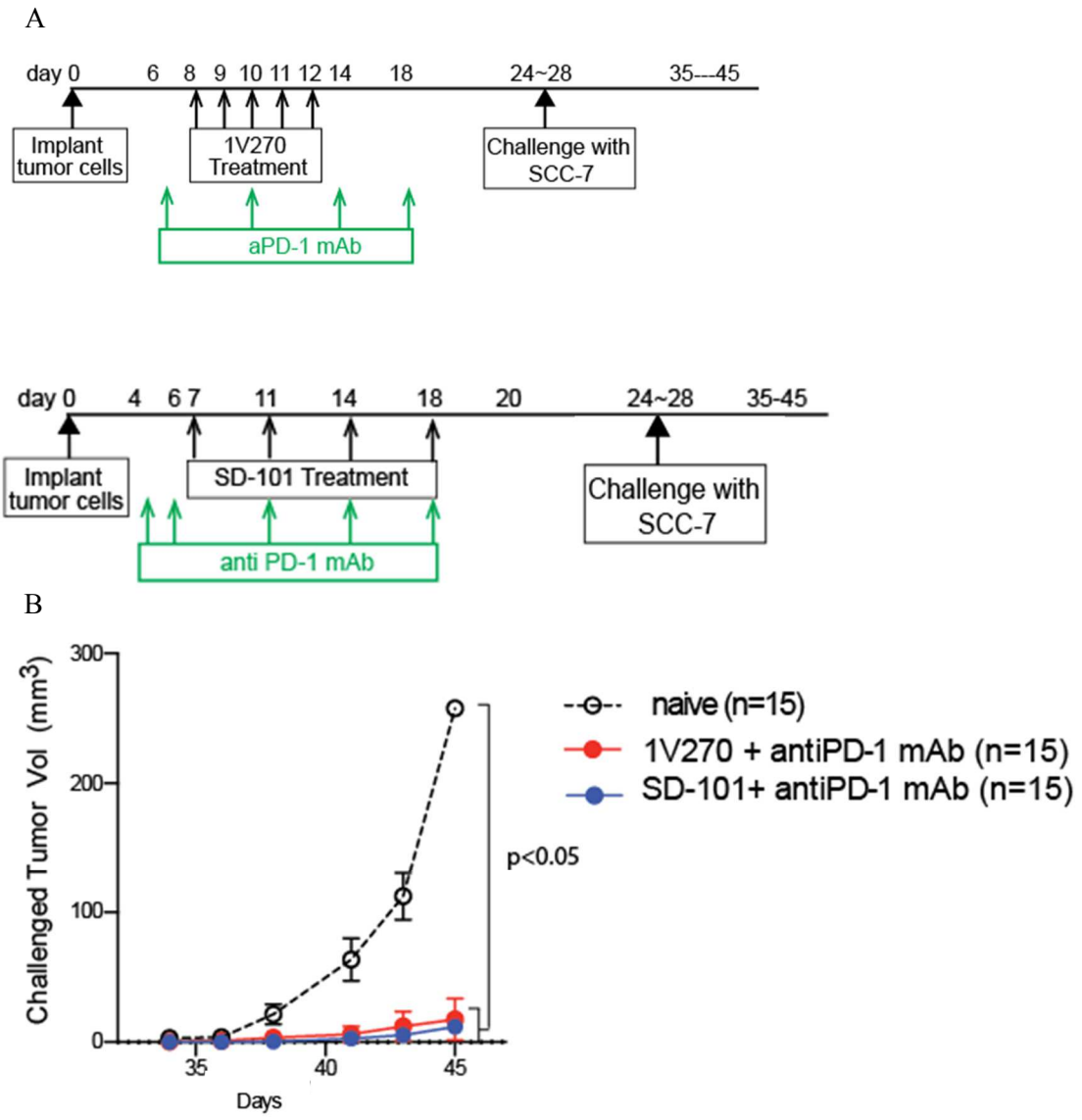

Figure 5: Treatment of anti-PD-1 with1V270 or SD-101 reduces subsequent tumor sizes**.** (A) Treatment protocol. Wild type female C3H/HeOuJ mice were inoculated with $1x10^5$ SCC-7 s.c. on right flanks on day 0. Two groups of mice (n=15) were treated with either 1V270 (100ug) i.t. on days 8, 9, 10, 11, and 12 and anti-PD-1 antibody (250ug) i.p. on days 6, 10, 14, and 18 or treated with SD-101 (50ug) i.t. on days 7, 11, 14, 18 and anti-PD-1 antibody (250 ug) i.p. on days 4, 6, 11, 14, and 18. An age-matched naïve group (n=15) served as a positive control. (B) Tumor lengths and widths were recorded over days post inoculation and tumor volumes were calculated using the formula $\frac{width\ x\ width\ x\ length}{2}$ and graphed using Prism software (version 6.0, GraphPad Software, Inc., San Diego, CA) and fitted by nonlinear regression. p value was calculated using one-way Anova. p value < 0.05 was considered statistically significant.

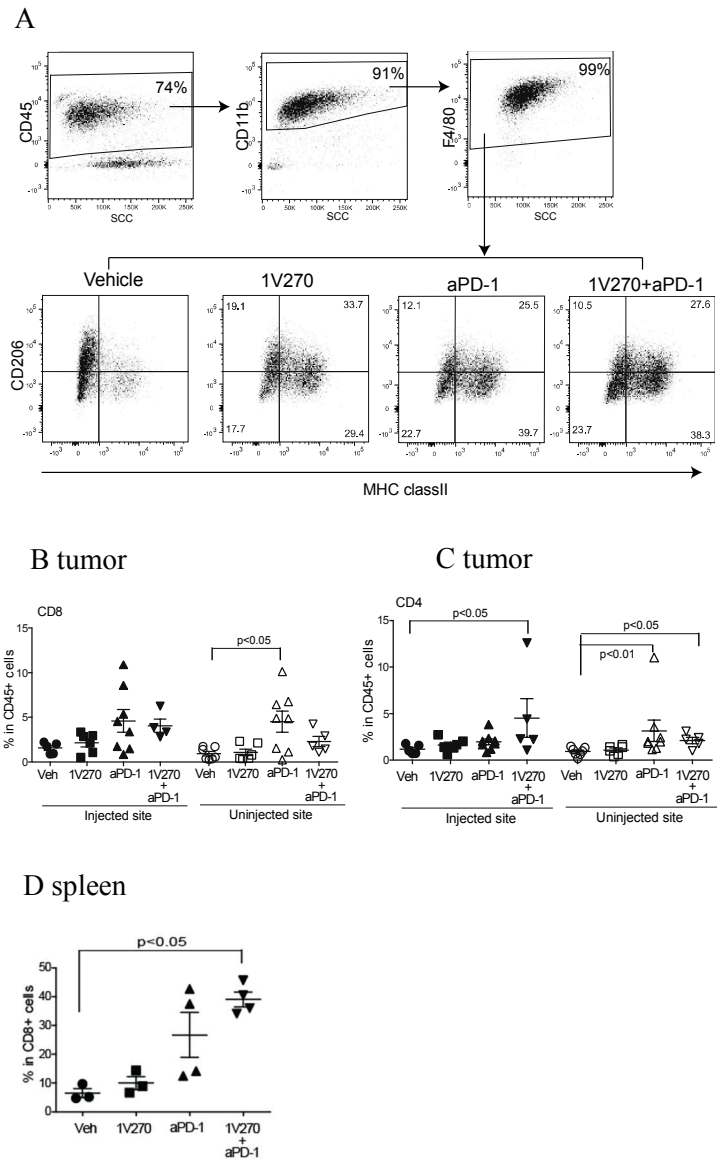

Figure 6: 1V270, anti-PD-1, and a combination increase M1/M2 macrophage ratio in the tumor microenvironment and $CD8^+$ T cell population in the spleen. Tumor samples were collected day 21, 9 days after the last injection of 1V270 following protocol in figure 3a (n=4). (A) FACS analysis of tumor infiltrating immune cells taken after treatment with vehicle, 1V270, anti-PD-1, and a combination. $CD45^+CD11b^+F4/80^+$ identifies macrophage population. M1-type and M2-type macrophages were identified as $CD206^{low}$ MHC class II^{high} and $CD206^{high}$ MHC class II^{low} respectively. Each number indicates % population in the gated parent population. (B) Levels of $CD8^+$ and $CD4^+$ T cells were graphed and compared between different treatments in injected tumor site versus uninjected tumor site. (C) The $CD8^+$ T cell population was graphed between different treatment groups in the spleen. p value was calculated using one-way Anova. p value < 0.05 was considered statistically significant.

A

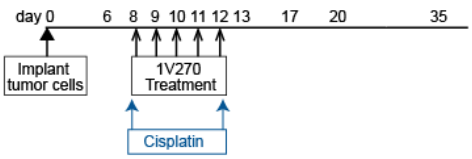

B

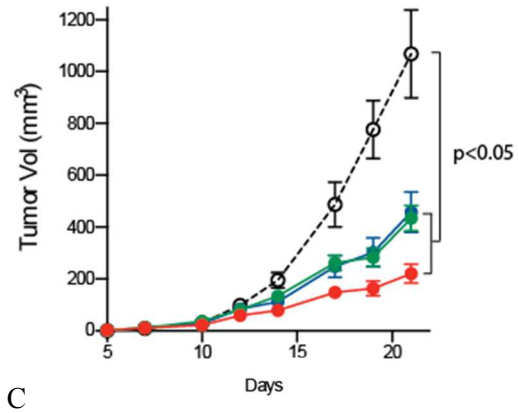

C

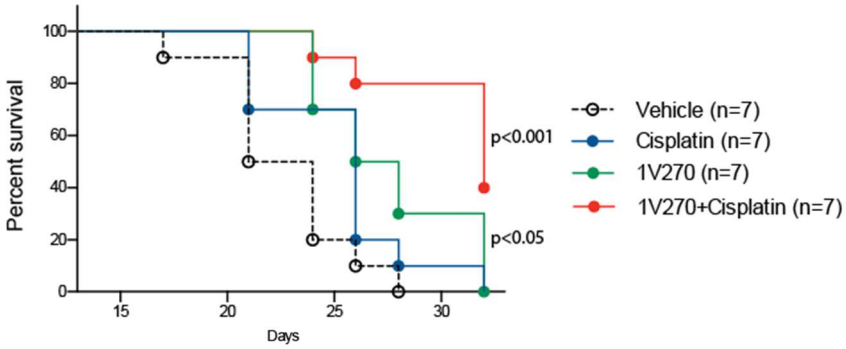

Figure 7: Treatment of 1V270 with cisplatin reduces local tumor sizes. (A) Treatment protocol. Wild type female C3H/HeOuJ mice were inoculated with $1x10^5$ SCC-7 s.c. on their right flanks on day 0. 1V270 (100ug) was administered i.t. on days 8, 9, 10, 11, and 12 and cisplatin (5mg/kg) was administered i.p. on days 8 and 12. (B) Tumor lengths and widths were recorded over days post inoculation and tumor volumes were calculated using the formula $\frac{width\ x\ width\ x\ length}{2}$ and graphed using Prism software (version 6.0, GraphPad Software, Inc., San Diego, CA) and fitted by nonlinear regression. p value was calculated using one-way Anova. C) Survival curve was graphed using Kaplan-Meier model. p value was calculated using log rank test. p value < 0.05 was considered statistically significant.

A

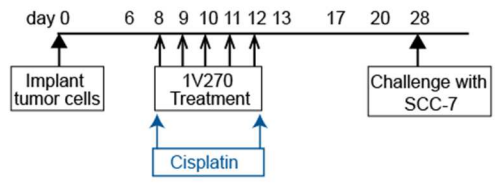

B

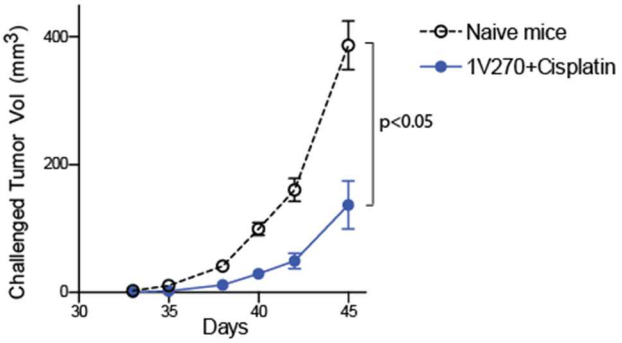

Figure 8: Treatment of 1V270 with cisplatin reduces subsequent tumor sizes. (A) Treatment protocol. Wild type female C3H/HeOuJ mice were inoculated with $1x10^5$ SCC-7 s.c. on their right flanks on day 0. 1V270 (100ug) was administered i.t. on days 8, 9, 10, 11, and 12 and cisplatin (5mg/kg) was administered i.p. on days 8 and 12. Mice were challenged with $1x10^5$ SCC-7 s.c. on left flanks on day 28 along with a naïve group of mice that served as a positive control. (B) Tumor lengths and widths were recorded over days post inoculation and tumor volumes were calculated using the formula $\frac{width\ x\ width\ x\ length}{2}$ and graphed using Prism software (version 6.0, GraphPad Software, Inc., San Diego, CA) and fitted by nonlinear regression. p value was calculated by two tailed student t test. p value < 0.05 was considered statistically significant.

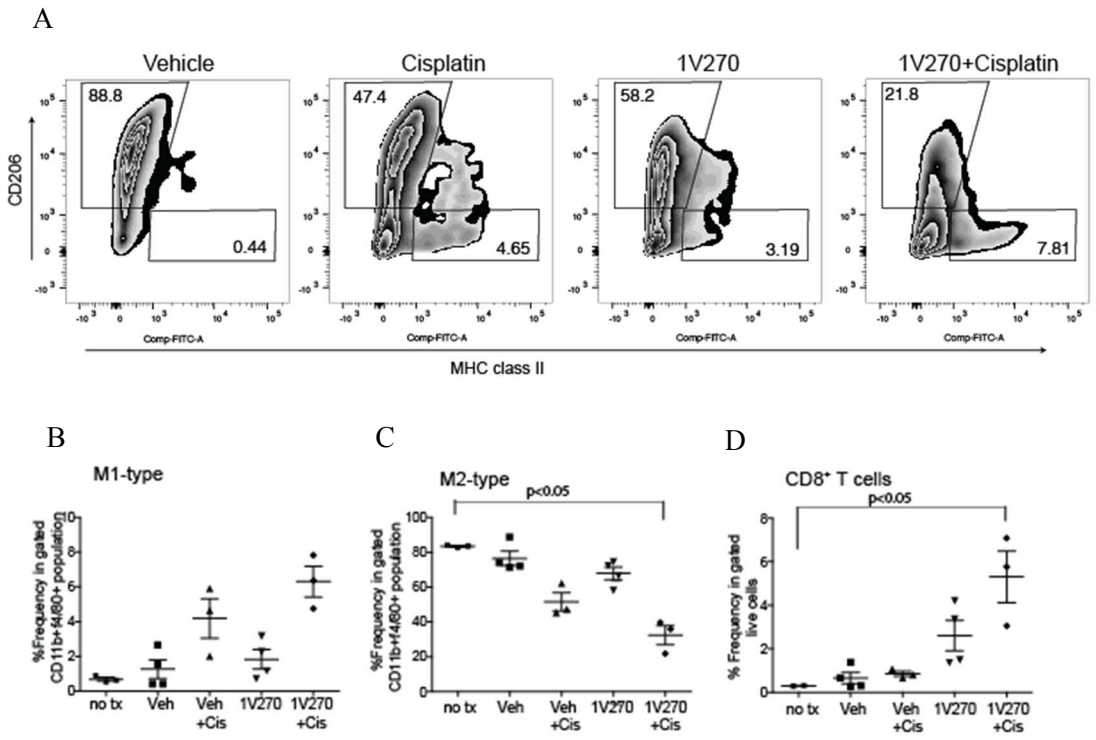

Figure 9: 1V270, cisplatin, and a combination increase M1/M2 macrophage ratio and $CD8^+$ T cell population in the tumor microenvironment. Protocol was the same as figure 7a. (A) FACS analysis of tumor infiltrating immune cells taken after treatment with vehicle, cisplatin, 1V270, or 1V270 and cisplatin. $CD45^+CD11b^+$ $F4/80^+$ identifies macrophage population. M1-type and M2-type macrophages were identified as $CD206^{low}$ MHC class II^{high} and $CD206^{high}$ MHC $classII^{low}$ respectively. Each number indicates % population in the gated parent population. (B) M1 macrophage frequencies between different treatment groups. (C) M2 macrophage frequencies between different treatment groups. (D) $CD8^+$ T cell frequencies in TIL between different treatment groups. p value was calculated using one-way Anova. p value < 0.05 was considered statistically significant.

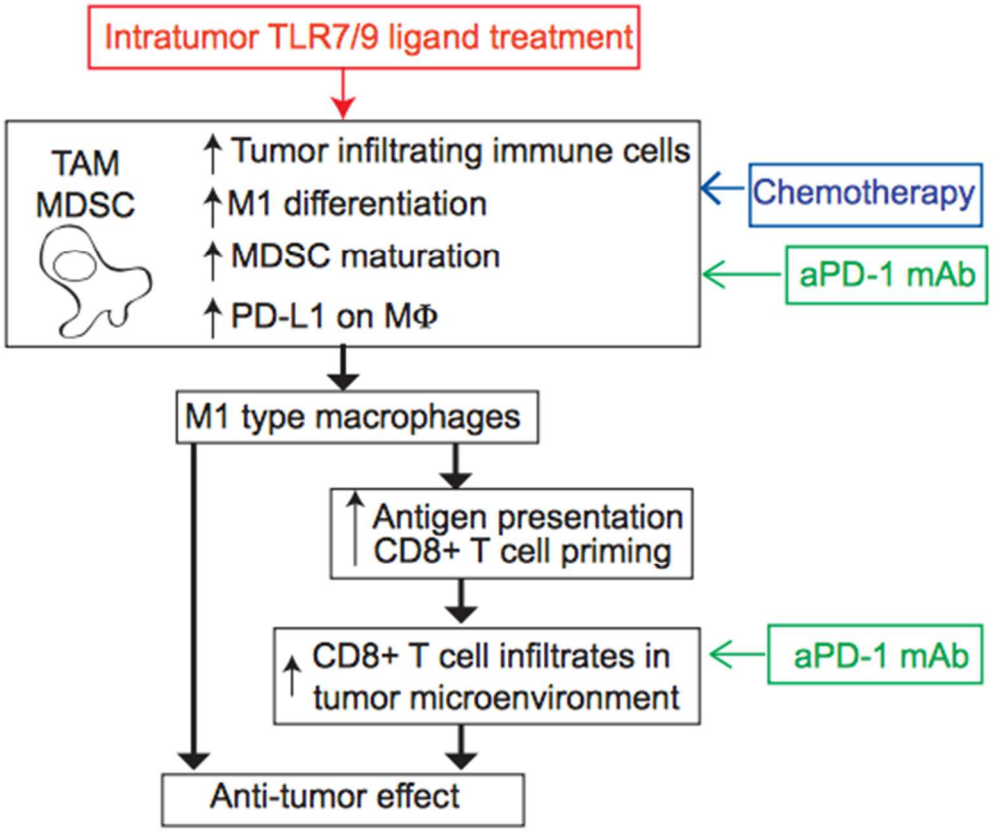

Figure 10: Proposed immuno-chemotherapy mechanism of action. In the proposed mechanism, chemotherapy is administered with TLR7 and TLR9 ligand treatment causing immune cells to infiltrate the tumors and M1 differentiation. anti-PD-1 antibody is administered and can prevent anti-PD-1 from binding to anti-PD-1 ligand in the periphery phase. Thus, the negative feedback of the immune system is inhibited leading to anti-tumor effects.

REFERENCES

[1] National Cancer Institute. (February 1, 2013). Head and Neck Cancers. http://www.cancer.gov/types/head-and-neck/head-neck-fact-sheet

[2] Lewis, Aaron, Kang, R., Levine, A., Maghami, E. (2015). The New Face of Head and Neck Cancer. The HPV Epidemic. Cancer Network.

[3] Mroz, E.A., Tward, A.D., Hammon, R.J., Ren, Y., Rocco, J.W. Intra-tumor genetic heterogeneity and mortality in head and neck cancer: analysis of data from Cancer Genome Atlas. PLOS Medicine. 12.

[4] Michor, F., Polyak, K. (2010). The Origins and Implications of Intratumor Heterogeneity. Cancer Prevention Research. 3, 1361.

[5] Cluman, R., Mohr, C., Kroger, K., Dost, P. (2007). The forearm flap: assessment of functional and aesthetic outcomes and quality of life. American Journal of Otolaryngology. 28, 367-374.

[6] Schoenfeld, J.D. (2015). Immunity in Head and Neck Cancer. Cancer Immunology Research. 3, 12.

[7] Vermorken, J.B., Spencenier, P. (2010). Optimal treatment for recurrent/metastatic head and neck cancer. Annals of Oncology. 21, 252-261.

[8] Most, R.G., Robinson, B.W., Lake, R.A. (2009). Combining Immunotherapy With Chemotherapy to Treat Cancer. Discovery Medicine. 5, 265-270.

[9] Zarour, H., DeLeo, A., Finn, O.J., Storkus, W.J. (2003). Categories of Tumor Antigens. Holland-Frei Cancer Medicine. 6th edition.

[10] Yim, E., Park, J. (2005). The Role of HPV E6 and E7 Oncoproteins in HPV-associated Cervical Carcinogenesis. Cancer Research and Treatment. 37, 319-324.

[11] Tang, D., Kang, R., Zeh, H.J., Lotze, M.T. (2011). High-mobility Group Box 1 [HMGB1] and Cancer. Biochimica et Biophysica Acta. 1799, 131.

[12] Peterson, T.R., Dickgreber, N., Hermans, I.F. Tumor antigen presentation by dendritic cells. (2010). Critical Reviews in Immunology. 30, 345-386.

[13] Adams, S. (2010). Toll-like receptor agonists in cancer therapy. Immunotherapy. 1, 949-964.

[14] Basu, A., Krishnamurthy, S. (2010). Cellular Responses to Cisplatin-Induced DNA Damage. Journal of Nucleic Acids. 2010, 16.

[15] Rabinovich, G.A., Gabrilovich, D., Sotomayor, E.M. Immunosuppressive strategies that are mediated by tumor cells. (2007). Annual Review of Immunology. 25, 267-296.

[16] Lebrun, J. (2012). The Dual Role of TGFβ in Human Cancer: From Tumor Suppression to Cancer Metastasis. International Scholarly Research Notices. 2012, 28.

[17] Couper, K.N., Blount, D.G., Riley, E.M. (2008). IL-10: The Master Regulator of Immunity to Infection. The Journal of Immunology. 180, 5771-5777.

[18] Duray, A., Demoulin, S., Hubert, P., Delvenne, P., Saussez, S. (2010). Immune Suppression in Head and Neck Cancers: A Review. Journal of Immunology Research. 15.

[19] Chanmee, T., Ontong, P., Konno, K., Itano, N. (2014). Tumor-Associated Macrophages as Major Players in the Tumor Microenvironment. Cancers. 6, 1670-1690.

[20] Stein, M., Keshav, S., Harris, N., Gordon, S. (1992). Interleukin 4 potently enhances murine macrophage mannose receptor activity: a marker of alternative immunologic macrophage activation. The Journal of Experimental Medicine. 176, 287-292.

[21] Yaddanapudi, K., Putty, K., Rendon, B.E., Lamont, G.J., Faughn, J.D., Satoskar, A., Lasnik, A., Eaton, J.W., Mitchell, R.A. (2013). Control of tumor-associated macrophage alternative activation by MIF. The Journal of Immunology. 190, 2984-2993.

[22] Mantovani A, Sozzani S, Locati M, Allavena P, Sica A. (2002). Macrophage polarization: tumor-associated macrophages as a paradigm for polarized M2 mononuclear phagocytes. Trends Immunol. 23,549–555.

[23] Kato, H., Watanabe, M. (2015). Myeloid-Derived Suppressor Cells and Therapeutic Strategies in Cancer. Mediators of Inflammation. 2015, 12 pages.

[24] Takeda, K., Kaisho, T., Akira, S. (2003). Toll-like Receptors. Annual Review of Immunology. 21, 335-376.

[25] Muzio, M., Mantovani, A. (2000). Toll-like receptors. Microbes and Infection. 2, 251-255.

[26] Hennessy, E.J., Parker, A.E., O'Neill, L. (2010). Box 1 TLR expression and ligand specificity. Nature Reviews. 9, 293-307.

[27] Frenzel, H., Hoffmann, B., Brocks, C., Schlenke, P., Pries, R., Wollenberg, B. (2006). Toll like receptor interference in myeloid dendritic cells through head and neck cancer. Anticancer Research. 26, 4409-4413.

[28] Hayashi, T., Chan, M., Norton, J.T., Wu, C.C.N., Yao, S., Cottam, H.B., Tawatao, R.I., Corr, M., Carson, D.A., Daniels, G.A. (2011). Additive melanoma suppression with intralesional phospholipid conjugated TLR7 agonists and systemic IL-2. Melanoma Research. 21, 66-75.

[29] Chan, M., Hayashi, T., Kuy, C.S., Gray, C.S., Wu, C.N., Corr, M., Wrasidlo, W., Cottam, H.B., Carson, D.A. (2009). Synthesis and Immunological Characterization of Toll-Like Receptor 7 Agonist Conjugates. Bioconjugate Chemistry. 20, 1194-1200.

[30] Krieg, A.M. (2008). Toll-like receptor 9 (TLR9) agonists in the treatment of cancer. Oncogene. 27, 161-167.

[31] (2015). Dynavax Presents Clinical Data From Lead Cancer Immunotherapy Candidate, SD-101, at ASH Annual Meeting. Dynavax Technologies.

[32] Warner, N., Nunez, G. (2013). MyD88: A Critical Adaptor Protein in Innate Immunity Signal Transduction. The Journal of Immunology. 190, 3-4.

[33] Calvano, S.E., Xiao, W., Richards, D.R., Felciano, R.M., Baker, H.V., Cho, R.J., Chen, R.O., Brownstein, B.H., Cobbs, J.P., Tschoeke, S.K., Graziano, C.M., Moldawer, R.W., Tompkins, R.G., Lowry, S.F. (2005). A network-based analysis of systemic inflammation in humans. Nature. 437, 1032-1037.

[34] Zhou, Q., Xiao, H., Liu, Y., Peng, Y., Hong, Y., Yagita, H., Chandler, P., Munn, D.H., Mellor, A., Fu, N., He, Y. (2010). Blockade of Programmed Death-1 Pathway Rescues the Effector Function of Tumor-Infiltrating T Cells and Enhances the Antitumor Efficacy of Lentivector Immunization. The Journal of Immunology. 185, 5082-5092.

[35] Intlekofern A.M., Thompson, C.B. (2013). At the Bench: Preclinical rationale for CLTA-4 and PD-1 blockade as cancer immunotherapy. Journal of Leukocyte Biology. 94, 25-39.

[36] McCoy, K.D., Gros, G.L. (1999). The role of CTLA-4 in the regulation of T cell immune responses. Immunology & Cell Biology. 77, 1-10.

[37] Kong, Y.M., Flynn, J.C. (2014). Opportunistic Autoimmune Disorders Potentiated by Immune-Checkpoint Inhibitors Anti-CTLA-4 and Anti-PD-1. Frontiers in Immunology. 5, 206.

[38] Smith, L.P., Thomas, G.R. (2005). Animal models for the study of squamous cell carcinoma of the upper aerodigestive tract: A historical perspective with review of their utility and limitations. Part A. Chemically-induced *de novo* cancer, syngeneic animal models of HNSCC, animal models of transplanted xenogeneic human tumors. International Journal of Cancer. 118, 2111-2122.

[39] Hoover, A.C., Spanos, W.C., Harris, G.F., Anderson, M.E., Klingelhutz, A.J., Lee, J.H. (2007). The role of human papilloma virus 16 E6 in anchorage independent and invasive growth of tonsil epithelium. JAMA Otolaryngology-Head & Neck Surgery. 133, 495-502.

[40] Anderson, A.S., Solling, A.S., Ovesen, T., Rusan, M. (2013). The interplay between HPV and host immunity in head and neck cell carcinoma. International Journal of Cancer. 134, 2755-2763.

[41] Engel, A.L., Holt, G.E., Lu, H. (2012). The pharmacokinetics of Toll-like receptor agonists and the impact on the immune system. Expert Review of Clinical Immunology. 4, 275-289.

[42] Wu, C.C., Crain, B., Yao, S., Sabet, M., Lao, F.S., Tawatao, R., Chan, M., Smee, D.F., Julander, J.G., Cottam, H.B., Guiney, D.G., Corr, M., Carson, D.A., Hayashi, T. (2014). Journal of Innate Immunity. 6, 315-324.

[43] Dynavax Technologies Corporation. A Trial of Intratumoral Injections of SD-101 in Combination With Pembrolizumab in Patients With Metastatic Melanoma. In: ClinicalTrials.gov [Internet]. Bethesda (MD): National Library of Medicine (US). 2016. Available from: https://clinicaltrials.gov/ct2/show/NCT02521870 NLM Identifier: NCT02521870.

[44] Broad, A., Jones, D.E., Kirby, J.A. Toll-like receptor (TLR) response tolerance: a key physiological "damage limitation" effect and an important potential opportunity for therapy. (2006). Current Medicinal Chemistry. 13, 2487-2502.

[45] Cullen, S.P., Brunet, M., Martin, S.J. (2010). Granzymes in cancer and immunity. Cell Death & Differentiation. 17, 616-623.

[46] Adrian, C., Murphy, B.M., Martin, S.J. (2004). Molecular Ordering of the Caspase Activation Cascade Initiated by the Cytotoxic T Lymphocyte/Natural Killer (CTL/NK) Protease Granzyme B. The Journal of Biological Chemistry. 280, 4663-4673/

[47] Zhu, J., Huang, X., Yang, Y. (2009). The TLR9-MyD88 pathway is critical for adaptive immune responses to adeno-associated virus gene therapy vectors in mice. The Journal of Clinical Investigation. 119, 2388-2398.

[48] Puiq, M., Tosh, K.W., Schramm, L.M., Graijkowska, L.T., Kirschnman, K.D., Tami, C., Beren, J., Rabin, R.L., Verthelyi, D. (2012). TLR9 and TLR7 agonists mediate distinct type I IFN responses in humans and nonhuman primates in vitro and in vivo. Journal of Leukocyte Biology. 91, 147-158.

[49] Krutziki, S.R., Tan, B., Li, H., Ochoa, M.T., Liu, P.T., Sharfstein, S.E., Graeber, T.G., Sieling, P.A., Liu, Y., Rea, T.H., Bloom, B.R., Modlin, R.L. (2005). TLR activation triggers the rapid differentiation of monocytes into macrophages and dendritic cells. Nature Medicine. 11, 653-660.

[50] Ferlito, A., Shaha, A.R., Silver, C.E., Rinaldo, A., Mondin, V. (2001). Incidence and sites of distant metastases from head and neck cancer. Journal for oto-rhino-laryngology and its related species. 63, 202-207.

[51] Biswas, S.K., Mantovani, A. (2010). Macrophage plasticity and interaction with lymphocyte subsets: cancer as a paradigm. Nature Immunology. 11, 889-896.

[52] Fairweather, D., Chihakova, D. (2009). Alternatively activated macrophages in infection and autoimmunity. Journal of Autoimmunity. 33, 222-230.

[53] Mantovani, A., Sica, A., Sozzani, S., Allavena, P., Vecchi, A., Locati, M. (2004). The chemokine system in diverse forms of macrophage activation and polarization. Trends in Immunology. 25, 677-686.

[54] Sindrilaru, A., Peters, T., Wieschalka, S., Baican, C., Baican, A., Peter, H., Hainzl A., Schatz, S., Qi, Y., Schlecht, A., Weiss, J.M., Wlaschek, M., Sunderkotter, C., Scharffetter-Kochanek, K. (2011). An unrestrained proinflammatory M1 macrophage population induced

by iron impairs wound healing in humans and mice. The Journal of Clinical Investigation. 121, 985-997.

[55] Wang, N., Liang, H., Zen, K. (2014). Molecular Mechanisms That Influence the Macrophage M1-M2 Polarization Balance. Frontiers in Immunology. 5, 614.

[56] Chen, W., Wang, J., Jia, L., Liu, J., Tian, Y. (2016). Attenuation of the programmed cell death-1 pathway increases the M1 polarization of macrophages induced by zymosan. Cell Death & Disease. 7.

[57] Flavell, R.A., Sanjabi, S., Wrzesinski, S.H., Licona-Limon, P. (2014). The polarization of immune cells in the tumor environment by TGFβ. Nature Reviews Immunology. 10.

[58] Spurrel, E.L., Lockley, M. (2014). Adaptive immunity in cancer immunology and therapeutics. ecancermedicalscience. 8, 441.

[59] Vallentin, B., Balogis, V., Piperoglou, C., Cypowyi, S., Zucchini, N., Chene, M., Navarro, F., Farnarier, C., Vivier, E., Vely, F. (2015). Innate Lymphoid Cells in Cancer. Cancer Immunology Research. 3, 1109-1114.

[60] Hadrup, S., Donia, M., Straten, P.T. (2012). Effector CD4 and CD8 T cells and Their Role in the Tumor Microenvironment. Cancer Microenvironment. 6, 123-133.